Production of Oxymethylene Dimethyl Ether from Hydrogen and Carbon Dioxide – Part I: Modeling and Analysis for OME1

Journal:	*Industrial & Engineering Chemistry Research*
Manuscript ID	ie-2018-05576g.R1
Manuscript Type:	Article
Date Submitted by the Author:	21-Feb-2019
Complete List of Authors:	Bongartz, Dominik; Rheinisch Westfalische Technische Hochschule Aachen, AVT.SVT Burre, Jannik; Rheinisch Westfalische Technische Hochschule Aachen, Process Systems Engineering (AVT.SVT) Mitsos, Alexander; Rheinisch Westfalische Technische Hochschule Aachen, AVT.SVT

Production of Oxymethylene Dimethyl Ether from Hydrogen and Carbon Dioxide – Part I: Modeling and Analysis for OME_1

Dominik Bongartz,† Jannik Burre,† and Alexander Mitsos*,‡,†,¶

†*Process Systems Engineering (AVT.SVT), RWTH Aachen University, 52074 Aachen, Germany*

‡*JARA-ENERGY, 52056 Aachen, Germany*

¶*Energy Systems Engineering (IEK-10), Forschungszentrum Jülich, 52425 Jülich, Germany*

E-mail: amitsos@alum.mit.edu

Phone: +49 241 80 94704. Fax: +49 241 80 92326

Abstract

Oxymethylene dimethyl ethers (OME_n) are potential compression ignition fuels or blend components that enable drastic reductions in pollutant formation. By combining multiple conversion steps, OME_n can be produced from carbon dioxide (CO_2) and hydrogen (H_2), and hence from renewable electricity. However, established processes for OME_n production are challenging to model and detailed analyses of OME_n production from H_2 and CO_2 are not yet available in the open literature. In the first part of our two-part article, state-of-the-art models for the formaldehyde-containing mixtures involved in OME_n production are implemented in AspenPlus and used to analyze a process chain for production of OME_1 from H_2 and CO_2 via methanol and aqueous formaldehyde solution. The exergy efficiency of the process chain is 73 %. Tailored

processes aiming at improved heat and mass integration as well as novel synthesis routes leading to reduced process complexity or avoiding oxidative intermediate steps hold significant promise for future efficiency improvements.

1 Introduction

Sustainable solutions for replacing fossil fuels in the transport sector are desperately needed to address the large contribution of transport-related greenhouse gas emissions to climate change.[1] Because of the large potential of renewable power sources, the use of renewable electricity in transportation holds significant promise in this respect. While battery electric vehicles are an attractive option for short-distance transportation, high energy density fuels are likely to be required for long-distance applications for the foreseeable future.[2]

In this context, conversion of renewable electricity to gaseous or liquid fuels (also called *e-fuels* or *electrofuels*) could be a promising alternative. Such fuel production (also termed *Power-to-Gas*, *Power-to-Liquid*, or more generally *Power-to-Fuel*) could also enhance the use of fluctuating renewable electricity in case it is adapted to the temporal and spatial distribution of wind and solar power generation,[3] as well as serve as a means for long-term energy storage.[4] Regarding the fuels to be produced from renewable electricity, various options are being discussed in literature[5] that differ in various aspects related to both production and vehicle application.[6]

Beyond greenhouse gas emissions, pollutant emissions of conventional power trains are eliciting increasing concern because of adverse health effects, in particular compression ignition (CI) engines fueled with fossil diesel fuel. Several alternative fuels exhibit the potential to significantly reduce pollutant formation compared to the conventional fossil fuels in addition to reducing greenhouse gas emissions.[6] Among these, oxymethylene dimethyl ethers (OME_n) have attracted particular attention recently[7,8] because of their potential to drastically reduce formation of soot and (through adapted engine calibration) nitrogen oxides (NO_x) in CI engines.[9,10] OME_n form a homologous series with the general formula $CH_3O(CH_2O)_nCH_3$.

The first member, OME_1, is also known as methylal or dimethoxymethane and has been shown to be an excellent blend component for fossil diesel.[9,11] Mixtures of higher OME_n, in particular those with $n = 3 - 5$, have properties similar to diesel fuel[12] and are considered both as blend components or as neat fuels.[7,10]

All common production pathways for OME_n proceed via methanol as an intermediate and contain multiple separate process steps.[13] Methanol in turn can be produced from hydrogen (H_2), which can be obtained from water electrolysis, and carbon dioxide (CO_2).[14] Thus, OME_n are potential e-fuels. While a variety of synthesis pathways and process concepts have been suggested in literature, analyses of an overall process chain for OME_n production are still scarce. Zhang et al.[15,16] present a process for the production of OME_n based on biomass gasification and analyze the influence of gasification conditions on OME_n formation. Schmitz et al.[17] analyze the cost of producing OME_1 and $OME_{3–5}$ from methanol and conclude that they can be cost competitive to fossil diesel fuel depending on oil and methanol prices. Ouda et al.[18],[19] present an alternative OME_n production process based on dehydrogenation of methanol to formaldehyde and conclude that it leads to lower production cost than the process analyzed by Schmitz et al.[17]. Mahbub et al.[20] and Deutz et al.[11] provide life cycle assessments for blends of fossil diesel with OME_n produced from biomass and of OME_1 produced from renewable electricity, respectively. They conclude that both pathways can yield significant reductions in life-cycle pollutant and (given suitable material and energy sources) greenhouse gas emissions compared to pure diesel.

However, these most existing process chain analyses rely on literature data on the separate process steps obtained from different sources[11,17,20] or are based on simplified assumptions regarding product separation.[15,16,18] Furthermore, detailed analyses of bottlenecks and points for improvements of a *Power-to-OME$_n$* process chain have not been presented. This is partly due to the fact that the thermodynamics of some of the mixtures involved are very challenging to model and so far have mostly been addressed with specialized models (e.g.,[21]) that are difficult to implement in commercial flowsheet simulators. Most existing detailed simulation

studies,[22,23] on the other hand, only consider single process steps and not the entire process chain.

Therefore, the purpose of this two-part paper is to conduct a detailed analysis of *Power-to-OME$_n$* process chains based on existing process steps to identify the potential and bottlenecks of the established concepts, and to provide model implementations that can serve as a starting point for the analysis and development of new process concepts using a commercial flowsheet simulator. In this first part, we consider the conversion of H_2 and CO_2 to OME_1, while in the second part we address the conversion to the longer chain $OME_{3\text{–}5}$.[24] In the following, we describe the process chain considered herein, discuss the thermodynamic models and their implementation in AspenPlus, and analyze the process chain with respect to potential points for improvement based on the simulation results. The model implementations are available via our homepage.[25]

2 Process Concepts

It is well established that OME_1 can be formed via reaction of methanol (MeOH) with formaldehyde (FA) in the presence of acid catalysts:[26]

$$2\text{MeOH} + \text{FA} \longrightarrow \text{OME}_1 + \text{H}_2\text{O}. \tag{R1}$$

While alternative synthesis pathways such as selective direct oxidation of methanol in the gas phase[27] or reaction of methanol with H_2 and CO_2 through homogeneous catalysis[28,29] have been suggested, these are at an earlier stage of development and are hence beyond the scope of this work.

We thus consider a process chain consisting of three existing process steps for converting H_2 and CO_2 to OME_1 via methanol and aqueous formaldehyde solution ($FA_{(aq)}$) as shown in Figure 1. By selecting existing process concepts that are based on well-studied reactions and separations or are even already applied industrially, we aim at analyzing the state of the

art and hence a short-term implementation option for *Power-to-OME$_1$*.

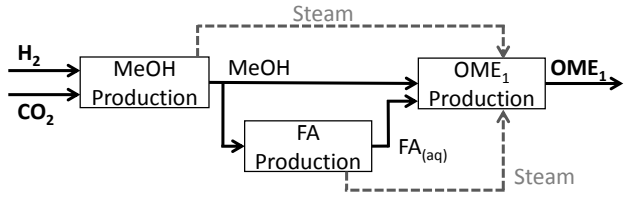

Figure 1: Block flow diagram of the considered process chain with base case heat integration.

As a base case, we consider the three process steps to be separate plants. We consider a hierarchical heat integration where each process step is heat-integrated, and additionally net excess heat from methanol and formaldehyde production is exported to the OME_1 production step (cf. Figure 1). This use of excess heat in the OME_1 production step either corresponds to the case where the three separate plants are located close enough together to actually exchange steam, or (in case the excess heat is actually exported to other processes not considered herein) it corresponds to a virtual exchange of steam that is accounted for in the net balance and hence overall efficiency. Alternatively, we also consider the case were the same processes are built as one single plant and are hence *fully* heat integrated, i.e., allowing all possible matches between heat exchangers located in different blocks in Figure 1.

2.1 Methanol Production

For methanol production, we consider a process based on the concepts of Pontzen et al.[30], Van-Dal and Bouallou[31] and Otto[32]. This is the same process that was considered in our previous comparison of other e-fuels[6] except that for the present analysis, the heat from the exothermic reaction and from combustion of the purge stream is not used for power generation but to generate steam at 30 bar to be exported to the OME_1 production step (see Figure 2). Hydrogen and CO_2 enter the process at ambient temperature and pressures of 30 bar and 1 bar, respectively, corresponding to the assumed pressures of electrolysis and CO_2 capture. The final product of this step is AA grade methanol with purity greater than 99.85 wt.-% and water content below 0.1 wt.-%.[33]

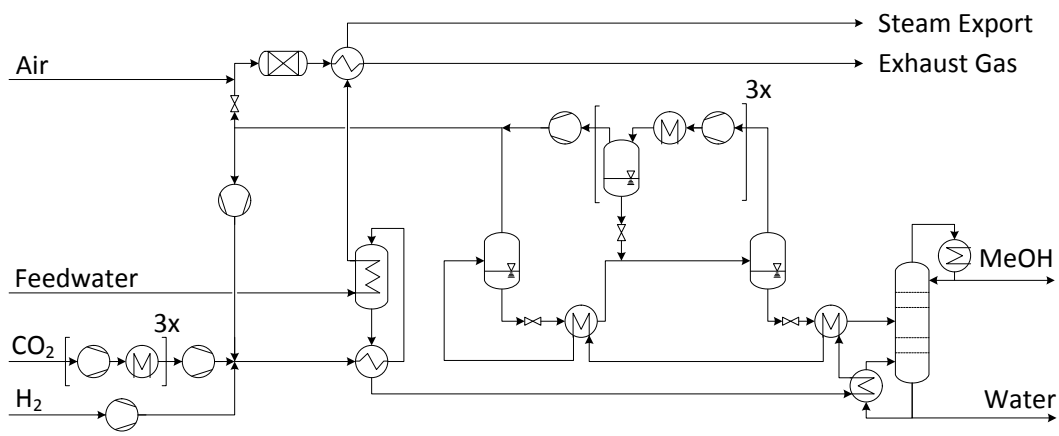

Figure 2: Process flow diagram for methanol production from H_2 and CO_2 based on the concepts of Pontzen et al.[30], Van-Dal and Bouallou[31] and Otto[32].

2.2 Formaldehyde Production

For formaldehyde production, we consider the BASF process as described by Reuss et al.[34] and Sperber[35] (see Figure 3). Methanol, air, and water enter the process at ambient pressure and temperature. They are evaporated, mixed with the recycle stream and fed to the reactor, where formaldehyde is formed in a combined partial oxidation and dehydrogenation over a silver catalyst in an adiabatic fixed bed reactor[34] according to the overall reactions

$$\mathrm{MeOH} \longrightarrow \mathrm{FA} + \mathrm{H_2}, \tag{R2}$$

$$\mathrm{H_2} + \frac{1}{2}\mathrm{O_2} \longrightarrow \mathrm{H_2O}. \tag{R3}$$

Note that (R2) and (R3) are selected for ease of modeling (cf. Section 3.2) since the actual partial oxidation reaction $\mathrm{MeOH} + \frac{1}{2}\mathrm{O_2} \longrightarrow \mathrm{FA} + \mathrm{H_2O}$ is a linear combination of (R2) and (R3) and is hence not needed in a conversion-based model. Main side reactions are the

formation of carbon monoxide (CO) and its oxidation to CO_2

$$\mathrm{MeOH} \longrightarrow \mathrm{CO} + 2\mathrm{H}_2, \tag{R4}$$

$$\mathrm{CO} + \frac{1}{2}\mathrm{O}_2 \longrightarrow \mathrm{CO}_2. \tag{R5}$$

The reactor effluent is rapidly quenched and fed to a four-stage absorption column where formaldehyde is separated from the product gas using water as a solvent to yield an aqueous formaldehyde solution of 50 wt.-% strength. The off-gas contains significant amounts of H_2 and CO and is hence burned in order to generate 5 bar steam in addition to that generated from the reactor effluent quenching.

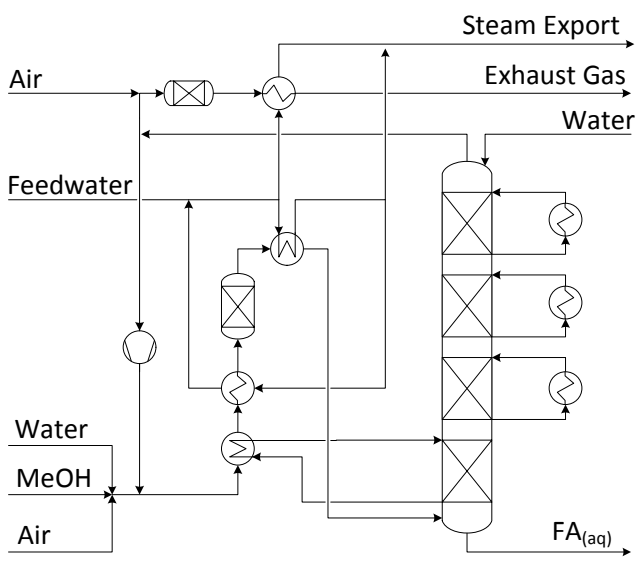

Figure 3: Process flow diagram for aqueous formaldehyde production from methanol via the BASF process as described by Reuss et al.[34] and Sperber[35].

2.3 OME_1 Production

For the OME_1 production step, a challenge lies in the purification of OME_1, which forms an azeotrope with methanol at high OME_1 contents.[36] To this end, different process concepts

have been suggested including extractive distillation,[37] two-pressure distillation,[38] or pervaporization.[39] For the present work, we consider the process developed by Weidert et al.[23,40,41] (see Figure 4). OME_1 is formed in the liquid phase in a fixed-bed reactor operating on an excess of methanol. A two-pressure distillation is used to overcome the azeotrope between methanol and OME_1. The first column additionally has a reactive section for converting remaining formaldehyde and a vapor side draw for removing methanol. Compared to the original concept,[23] we consider methanol recycling from the side draw of the first column to the reactor inlet. This stream is also used to preheat the reactants. Furthermore, we added a purge stream to avoid accumulation of non-condensables in an actual process and simplify numerical solution. The steam generated after combustion of this purge stream is used to reduce the heat demand of the second column.

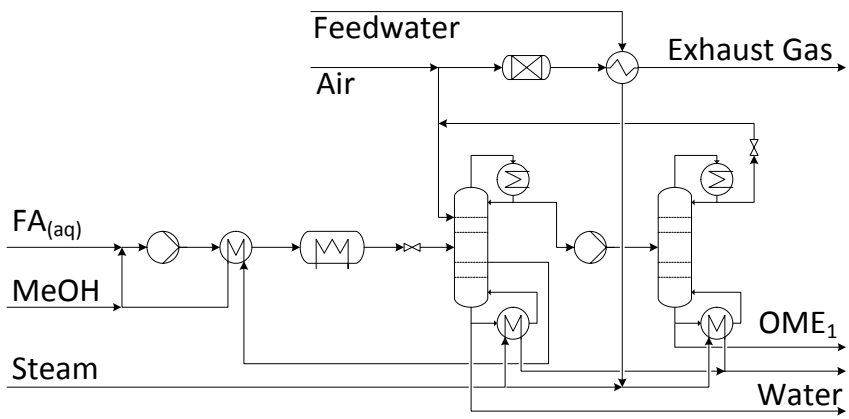

Figure 4: Process flow diagram for OME_1 production from methanol and aqueous formaldehyde based on the concept of Weidert et al.[23,40,41]

3 Modeling and Implementation

We implement models for the process steps described in Section 2 for converting H_2 and CO_2 to OME_1 in AspenPlus v8.8. This section summarizes the thermodynamic model used for formaldehyde-containing solutions and its implementation in AspenPlus, the process models for the three process steps, and the exergy calculations used to analyze the process chain.

3.1 Thermodynamic Model for Formaldehyde Solutions

A particular challenge lies in modeling the formaldehyde-containing mixtures involved in the last two process steps. Formaldehyde readily reacts with water to form methylene glycols (MG_n, $HO(CH_2O)_nH$)[26] according to the reactions

$$H_2O + FA \longleftrightarrow MG_1, \tag{R6}$$

$$MG_{n-1} + FA \longleftrightarrow MG_n, \quad n \geq 2, \tag{R7}$$

and with methanol to form hemiformals (HF_n, $CH_3O(CH_2O)_nH$)[26] according to the reactions

$$MeOH + FA \longleftrightarrow HF_1, \tag{R8}$$

$$HF_{n-1} + FA \longleftrightarrow HF_n, \quad n \geq 2. \tag{R9}$$

These reactions proceed quickly without any catalyst, and their equilibria are such that monomeric formaldehyde is only present in negligible amounts.[34] Therefore, these reactions also have a significant influence of phase equilibria and enthalpies of such mixtures[42] .

Maurer[43] presented the first model to explicitly account for both physical and chemical effects simultaneously for formaldehyde-containing mixtures. Besides the stable species H_2O, MeOH, and FA, in the liquid phase it considers the unstable species MG_n and HF_n up to a certain chain length. In the gas phase, on the other hand, it only considers MG_1 and HF_1, since the vapor pressure of the longer chain MG_n and HF_n with $n \geq 2$ is deemed sufficiently low for these species to remain in the liquid phase only. Equilibrium of reactions (R6)–(R9) in the liquid phase is enforced through acitivity-based equilibrium constants simultaneously with phase equilibrium based on the UNIFAC model.[44] For the latter, new groups are introduced for parts of the MG_n and HF_n.[43]

Many refined versions of this model have since been presented that contain improved parameter values based on additional experimental data,[45–48] introduce an enthalpy model,[49,50]

consider mixtures involving OME_1,[21,36] trioxane,[43,51] and higher OME_n,[52] use UNIQUAC[53] rather than UNIFAC for describing non-ideality in the vapor-liquid equilibria,[54] or rely on a kinetic rather than equilibrium description of reactions (R6)–(R9).[55] The resulting models can describe phase equilibria, enthalpies of vaporization, and the actual chain length distributions of methylene glycols and hermiformals in such mixtures with good accuracy.

However, the models are also rather complex and not straightforward to implement in commmercial flowsheet simulators. In the past, the models have sometimes be treated either in general purpose numerics software like MATLAB (e.g., Drunsel et al.[56]) or custom codes (e.g., Albert[57]). Some previous work has used flowsheet simulators like AspenPlus (e.g., Ott[58]) or MATLAB codes implementing a slightly different model coupled to CHEMCAD (Ouda et al.[19]). To our knowledge, none of these implementations are publicly available. For the present work, we reformulate the models slightly and implement them directly in AspenPlus as described in the following. The AspenPlus implementation of the models is available via our homepage.[25]

The species MG_n and HF_n for $n \leq 10$ are added as user-defined components in AspenPlus. Group contribution estimates from Ott[58] are used for the critical point of MG_n and HF_n. Antoine parameters for MG_1, HF_1 and OME_1 are taken from literature[36,48,59] while those for MG_n and HF_n with $n \geq 2$ are arbitrarily chosen to yield an extremely low vapor pressure ($< 10\,\mathrm{mbar}$) that effectively prevents them from entering the vapor phase. For the remaining species, critical point and vapor pressure data are taken from the AspenPlus database.

In accordance with the original models,[43] we consider an ideal vapor phase and describe nonideality of the liquid phase through the UNIFAC model, neglecting pressure dependence of the liquid phase fugacity. The UNIFAC groups and corresponding group and binary interaction parameters are taken from Kuhnert et al.[21]. However, Kuhnert et al.[21] use temperature-dependent correlations for binary interaction parameters between the UNIFAC groups representing water and OME_1, respectively, and those representing water and the CH_2OH group occuring in HF_n. Such temperature-dependent correlations are not available

in AspenPlus. Therefore, a simplification needs to be made for these pairs of groups. We simply evaluate the binary interaction parameters of Kuhnert et al.[21] at 300 K and implement the resulting values in AspenPlus. This is a limitation compared to the original model that should be kept in mind when applying it over a wide range of conditions. Nevertheless, we do not expect severe consequences for the present application. For the pair representing water and OME_1, the temperature dependence was originally introduced to describe the liquid-liquid equilibrium between water and OME_1 more accurately.[36] However, this liquid-liquid equilibrium does not occur at the conditions of interest (large amounts of methanol present), and the vapor-liquid equilibrium is reproduced well (cf. Supporting Information (SI)). The pair representing water and CH_2OH impacts activity coefficients in mixtures containing water, methanol, and formaldehyde. For such mixtures, the simplified model still predicts vapor pressures very well over a range of temperatures (cf. SI), while its predictions for the partition coefficient of formaldehyde are slightly less accurate at higher temperature than the original model[48] (cf. SI).

In order to account for reactions (R6)–(R9), they are implemented in the *Chemistry* section of AspenPlus, which is designed for electrolyte chemistry or other liquid phase equilibrium reactions. This way, these reactions can be enabled in any unit involving phase equilibrium. Parameters for activity-based equilibrium constants are taken from Drunsel[40].

The original enthalpy model[49,50,57] for computing pure component enthalpies of the MG_n and HF_n needs to be reformulated to enable implementation in AspenPlus, since it uses different calculations routes for different species. For example, in the original enthalpy model as presented by Albert[57], the calculation of the enthalpy of MG_n and HF_n for $n \geq 2$ proceeds via the liquid phase enthalpies of FA, H_2O, MeOH, MG_1 and HF_1, and the enthalpy of reaction of the chain growth reactions ($n \geq 2$)

$$\mathrm{MG_{n-1}} + \mathrm{MG_1} \longleftrightarrow \mathrm{MG_n} + \mathrm{H_2O}, \qquad (R7^*)$$

$$\mathrm{HF_{n-1}} + \mathrm{HF_1} \longleftrightarrow \mathrm{HF_n} + \mathrm{MeOH}, \qquad (R9^*)$$

which are considered instead of reactions (R7) and (R9) in several previous versions of the models.[43,57] Note, however, that due to linear dependency both descriptions ((R7) and (R9) vs. ($R7^*$) and ($R9^*$)) are equivalent in case of an equilibrium-based model. Herein, we reformulate the enthalpy model to correspond to the standard calculation route for pure component enthalpies in AspenPlus. Details on this procedure can be found in Section S2 of the SI.

In order to validate the model reformulation and implementation, we compare predictions from AspenPlus simulations to experimental data from literature. The validation results can be found in Section S3 of the SI. Note that for interpreting compositions it is often convenient to consider overall mole fractions of H_2O, MeOH, and FA (i.e., those in a fictitious mixture in which all MG_n and HF_n have been decomposed to H_2O, MeOH, and FA) rather than true mole fractions including the unstable MG_n and HF_n.[43] The experiments simulated for validation include (i) vapor liquid equilibria of mixtures of FA, H_2O, and MeOH (compared quantities are vapor pressure, saturation temperature, overall gas and liquid phase composition,[46–48] true liquid phase composition,[46] and enthalpy of vaporization[50]), (ii) liquid density of mixtures of FA, H_2O, and MeOH,[60,61] (iii) kinetics of OME_1 formation from MeOH and FA,[56] and (iv) distillative separation of H_2O, MeOH, FA, and OME_1.[40] Similar to the original model, the predictions agree well with the experimental data, with the restriction regarding temperature-dependence of binary interaction parameters discussed above.

3.2 Process Models

Models for all three process steps are implemented in AspenPlus using the thermodynamic model described in Section 3.1, except for the high-pressure recycle in the methanol production process, which is modeled using the Soave-Redlich-Kwong equation of state[62] with modified Huron-Vidal mixing rules.[63] For consistency, the assumptions regarding efficiencies of compressors and minimum temperature differences in heat exchangers are identical to those used in our previous analysis of other e-fuels.[6]

In the methanol production process (cf. Figure 2), the isothermal fixed bed reactor is modeled as a plug flow reactor using the kinetics presented by Van-Dal and Bouallou[31], who reformulated the original kinetic model of van den Bussche and Froment[64] for implementation in AspenPlus. The distillation is modeled using the RadFrac model with specifications based on Otto[32].

In the model of the formaldehyde production process (cf. Figure 3), the conversions of reactions (R2) and (R4) are adjusted to achieve 98 % methanol conversion at 90 % formaldehyde yield,[34] while those of reactions (R3) and (R5) are adjusted to meet the ratio of CO_2 to CO and H_2 to CO_2 in the off gas reported by Reuss et al.[34]. The exhaust gas recycle is adjusted to limit the reactor temperature to 700 °C. In the absorber, the water flow rate is chosen to yield a final product of 50 wt.-% formaldehyde. The cooling of the liquid circulating on the absorption column stages is chosen such that the lowest stage supplies the required heat for evaporating the reactor feed,[34] while the topmost stage operates at 35 °C to enable the use of cooling water. Since the process operates at atmospheric pressure, electrical power input is only required to drive fans for overcoming pressure drop. Lacking sufficient information for reliable computation of pressure drop, we use the electricity consumption reported by Sperber[35]. This electricity consumption is not included in the AspenPlus implementation but rather only taken into account for the subsequent evaluation of process performance.

In the OME_1 production step, the reactor is modeled using the kinetics presented by Drunsel et al.[56] for the reaction

$$\mathrm{MeOH} + \mathrm{HF}_1 \longleftrightarrow \mathrm{OME}_1 + \mathrm{H_2O} \tag{R10}$$

Since AspenPlus failed to converge the plug flow reactor with reaction (R10) when simultaneously considering equilibrium of the oligomerization reactions (R6)–(R9), the latter are disabled in the reactor. Even without considering equilibrium of reactions (R6)–(R9), agreement with the experimental data on OME_1 formation by Drunsel et al.[56] is good (cf. Section

S3.3 of the SI). This may, however, not hold in cases with much higher formaldehyde content in the reactant mixture (as could be, for example, encountered when producing longer chain OME_n from methanol and formaldehyde[65]) and this limitation should thus be kept in mind when using the present model implementations. Note that the reactor outlet composition differs somewhat from that reported by Weidert et al.[23] since we consider recycling of methanol from the first column, which still contains some water and hence shifts the reactant composition.

The distillation columns in the OME_1 production step are implemented as RadFrac models with kinetically-controlled reactive stages and a vapor side draw in the first column. To enable the use of the kinetics for OME_1 formation on the reactive stages (which contain the catalyst), the pre-exponential factor is converted to a holdup volume basis (rather than catalyst mass), and the associated holdup volume of the stages is taken based on the column specifications and catalyst data given by Drunsel[40]. The equilibrium reactions (R6)–(R9) are enabled for all stages of the first column except the catalyst-containing stages (because of the numerical difficulties in the plug flow reactor when considering equilibrium of (R6)–(R9) together with the kinetically controlled reaction (R10), cf. above). In the second column, reactions (R6)–(R9) are disabled since the formaldehyde content is negligible.

3.3 Efficiency Analysis

To analyze the potential for improvement and identify bottlenecks, we analyze the efficiency of the considered process chain using two different performance measures.

First, we consider the *chemical conversion efficiency* (cf., e.g.,[66])

$$\eta_{\mathrm{CCE}} = \frac{\dot{m}_{\mathrm{OME_1}} \cdot \mathrm{LHV}_{\mathrm{OME_1}}}{\dot{m}_{\mathrm{H_2}} \cdot \mathrm{LHV}_{\mathrm{H_2}}},$$

where $\mathrm{LHV_i}$ denotes the lower heating value. It differs from the first-law efficiency in that it does not account for heat or work transfer. Instead, η_{CCE} measures how much fuel energy

can be obtained from a given amount of H_2, which is the main energy source and cost driver[6] and hence likely to be a limiting factor in fuel production.

To account for heat and work input in a consistent manner, we also consider the exergy efficiency for the conversion of H_2 and CO_2 to OME_1 defined as

$$\eta_{\text{exergy}} = \frac{\dot{m}_{\text{OME}_1} \cdot e_{\text{OME}_1}}{\dot{m}_{\text{H}_2} \cdot e_{\text{H}_2} + \dot{m}_{\text{CO}_2} \cdot e_{\text{CO}_2} + P_{\text{el}} + \dot{E}_{\text{Q}}},$$

where $\dot{m}_{\text{i}}$ denotes the mass flow rate of stream i, e_{i} denotes the specific exergy, P_{el} denotes the electricity consumed by the process chain and $\dot{E}_{\text{Q}}$ denotes the sum of the exergy input associated with heat demand. The ambient temperature is set to 298 K. No distinction is made between exergy destruction and exergy losses to the environment (cf., e.g., Bejan et al.[67]), and for representation in the Sankey diagram, the sum of both is computed as the difference between the exergy of streams entering the process step and that of useful streams leaving the process steps.

The specific exergy of the material flows are computed as the sum of the physical exergy obtained from AspenPlus and the chemical exergy which is approximated here as the change in Gibbs free energy upon combustion at ambient conditions. We assume liquid water in the combustion products (i.e., compute the chemical exergy based on the higher heating value), corresponding to an environment model in which water is liquid (rather than gaseous in water-saturated air).[67] This choice is made since some process steps produce liquid water as a side product. If the chemical exergy was computed based on the lower heating value, it would thus underestimate the amount of useful energy that can be extracted in these process steps and the resulting exergy efficiencies could exceed unity. For aqueous formaldehyde solution, the enthalpy and entropy changes when dissolving gaseous formaldehyde in water are considered in addition to the chemical exergy of gaseous formaldehyde.

4 Results & Discussion

The specific raw material and energy demand as well as direct CO_2 emissions according to the simulations are given in Table 1. More details on the material and energy flows of the separate process steps can be found in the SI.

Table 1: Simulation results for relevant net mass and energy flow rates per unit mass of OME_1 produced.

Stream	Unit	Value
Input		
H_2	kg/kg_{OME_1}	0.264
CO_2	kg/kg_{OME_1}	1.92
Electricity	MJ/kg_{OME_1}	1.42
Heat (100 °C)	MJ/kg_{OME_1}	3.96
Output		
CO_2 (exhaust)	kg/kg_{OME_1}	0.118

4.1 Chemical Conversion Efficiency

The resulting chemical conversion efficiency (cf. Section 3.3) for the conversion of H_2 to OME_1 is 73 %. This is 9–17 percentage points lower than that of more commonly discussed e-fuels like methane (82 %), methanol (85 %), or DME (90 %).[6] However, while there are inherent differences between different fuels in their maximum achievable chemical conversion efficiencies,[6] this is not the reason for the lower value observed for OME_1.

In fact, a hypothetical process conducting the desired overall reaction (which, however, is not the ideal overall reaction of the present process, cf. below)

$$8\,H_2 + 3\,CO_2 \longrightarrow OME_1 + 4\,H_2O \tag{R10}$$

without any losses would achieve a chemical conversion efficiency of 91 % which is similar to the maximum achievable value for DME and better than those of methane or methanol.[6]

However, since established formaldehyde production processes like the BASF process considered herein are based on partial oxidation (or, if combined with a dehydrogenation, burn the generated H_2), the ideal overall reaction of the considered process chain (assuming perfect yield) is

$$9\,H_2 + 3\,CO_2 + \frac{1}{2}O_2 \longrightarrow OME_1 + 5\,H_2O, \tag{R11}$$

which would result in a conversion efficiency of 81 %. This is hence an upper bound for all OME_1 production processes relying on oxidative formaldehyde synthesis, since they are redox-inefficient.[11,28] The actual conversion efficiency of the present process (73 %) is lower still because of additional losses due to the side reactions in formaldehyde synthesis (cf. Section 2) and, to a lesser extent, purge streams and impurities in the byproduct streams of the three process steps.

4.2 Exergy Efficiency

The overall exergy efficiency for converting H_2 and CO_2 to OME_1 is also 73 %. Note that while it is numerically identical to the chemical conversion efficiency in this case, in general, the exergy efficiency can be either higher or lower, depending on how much additional process energy is needed and how efficiently chemical energy that is realeased in the process (in case of an exothermic overall reaction) is utilized. The present result, which is based on the process simulations, is in good agreement with the previous analysis based on literature data on the separate process steps, which predicts an efficiency of 74 %.[11]

The exergy efficiency is thus 13–17 percentage points lower than that of methane, methanol, or DME (87–91 %).[6] The Sankey diagram in Figure 5 demonstrates that losses accumulate throughout the process chain, which is more complex than the processes for producing the aforementioned other e-fuels. However, relative to the total exergy flows through the respective process steps, the largest exergy losses again arise in formaldehyde production. In fact, when comparing the exergy efficiencies of the separate process steps, the efficiency of the

formaldehyde production step (73 %) is significantly lower than that of the methanol (91 %) or final OME_1 (90 %) production steps. This can again partly be attributed to the conversion of high-quality chemical energy to thermal energy in the partial oxidation of methanol as well as the combustion of CO and H_2 in the off gas. Additional losses arise from the residual thermal energy of the exhaust gas and heat transfer over large temperature differences in product quenching as well as the heat recovery steam generator.

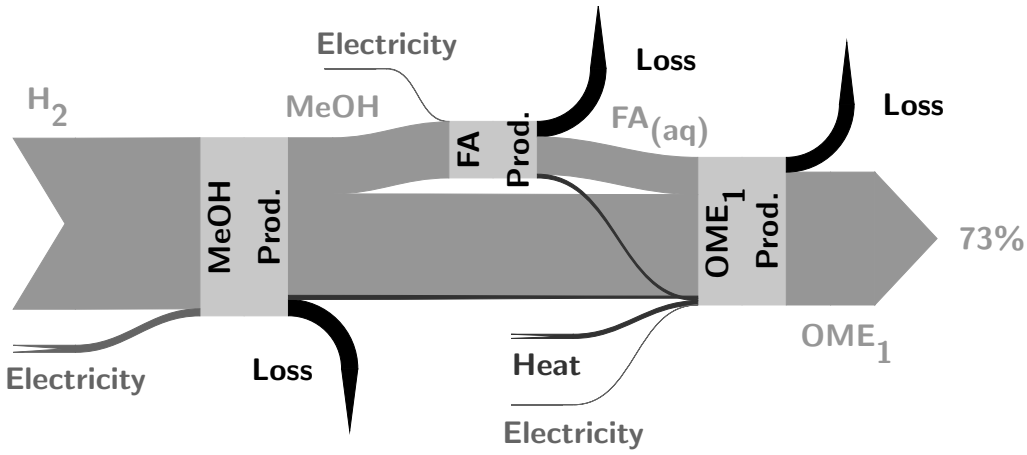

Figure 5: Sankey diagram of the benchmark process chain based on the simulation results. The width of the arrows is proportional to the exergy of the respective streams.

4.3 Heat Integration

In contrast to the other e-fuels mentioned above,[6] the composite process chain for OME_1 production has a net heat demand (cf. Table 1). Besides causing additional operating cost, this can also have a significant detrimental effect on the carbon footprint in case heat is supplied from fossil sources such as natural gas (cf. the worst-case scenario considered by Deutz et al.[11]). In case all three process steps are actually conducted in the same plant, one option for reducing this heat demand is to consider full heat integration across the entire process chain. To estimate the impact of such a measure, we conduct a pinch analysis considering all heat transfer required in the three process steps, and using the output temperatures of the intermediate products for the inputs of the following process steps. The

resulting grand composite curve is shown in Figure 6. Compared to the concatenation of three separate (heat integrated) plants with exchange of surplus steam, a complete heat integration can reduce the overall heat demand per unit mass of OME_1 by 63 % to 1.46 MJ/kg to be supplied at 80 °C. However, since the overall exergy efficiency is mainly dictated by the utilization of the energy in the feedstock H_2 (cf. Figure 5), the overall exergy efficiency only increases by about one percentage point to 74 %.

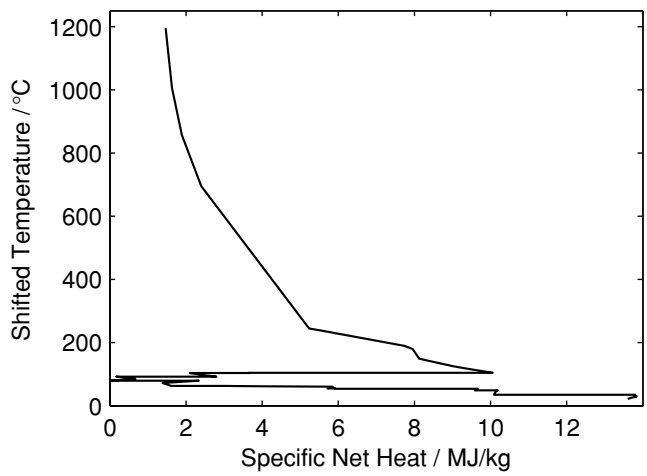

Figure 6: Grand composite curve for full heat integration of the entire process chain. Net heat flows are given per amount of OME_1 produced. Minimum temperature difference: 10 K.

5 Conclusion

We have implemented a detailed process model for the conversion of H_2 and CO_2 to OME_1 via methanol and aqueous formaldehyde in AspenPlus. The model implementations are available via our homepage.[25] They include an implementation of state-of-the-art thermodynamic models for formaldehyde-containing solutions. Because of the limited modeling flexibility of AspenPlus, certain simplifications needed to be made in the thermodynamic model that should be kept in mind when applying the models to conditions differing significantly from the ones considered herein.

The analysis of the process chain based on the simulation results confirms that production

of OME_1 from H_2 and CO_2 and hence from renewable electricity is possible through a combination of established process steps at reasonable efficiency. However, both the amount of fuel energy obtained from a given amount of H_2 and the overall exergy efficiency are still lower than those of other e-fuels such as methane, methanol, or dimethyl ether. This can be attributed to the complexity of the considered process chain with multiple reaction and separation steps, as well as the partial oxidation used in today's formaldehyde production processes. Thus, future developments should aim at more integrated processes and more direct synthesis pathways, in particular those avoiding the oxidative intermediate step.

As a first step towards closer integration, full heat integration of the process chain can reduce the overall heat demand by two thirds even compared to the base case of three separate heat integrated plants. While being a potentially important economic and environmental advantage, this has only a minor effect on overall efficiency. Further improvements could likely be achieved by optimizing the process chain as one single process, e.g., by tailoring separations to the requirements of downstream steps.

Finally, novel synthesis routes promise additional efficiency gains. In particular, the selective direct oxidation of methanol to OME_1 that has attracted increasing attention recently[27] could allow to merge two process steps with potential savings in equipment cost and separation energy. On the other hand, switching to formaldehyde production via dehydrogenation, as was recently suggested by Ouda et al.[19] for production of higher OME_n, could eliminate the losses due to partial oxidation, but would still require three process steps. Ultimately, a recently proposed purely reductive synthesis[28,29] from methanol, H_2, and CO_2 could combine both advantages and promise further efficiency gains still.[11] However, compared to the technologies considered herein, these alternatives are at a lower level of technical maturity and will require further development and analysis to assess their actual performance.

Acknowledgement

The authors gratefully acknowledge funding by the German Federal Ministry of Education and Research (BMBF) within the Kopernikus Project P2X: Flexible use of renewable resources – exploration, validation and implementation of 'Power-to-X' concepts. The authors also thank Maria A. Ortega Cardona for her support in implementing the models.

Supporting Information Available

Stream tables of the considered process chain. Derivation of the enthalpy model. Validation of the implemented thermodynamic models. This material is available free of charge via the Internet at `http://pubs.acs.org/`.

References

(1) Sims, R.; Schaeffer, R.; Creutzig, F.; Cruz-Núñez, X.; D'Agosto, M.; Dimitriu, D.; Figueroa Meza, M. J.; Fulton, L.; Kobayashi, S.; Lah, O.; McKinnon, A.; Newman, P.; Ouyang, M.; Schauer, J. J.; Sperling, D.; Tiwari, G. Transport. In *Climate Change 2014: Mitigation of Climate Change. Contribution of Working Group III to the Fifth Assessment Report of the Intergovernmental Panel on Climate Change*; Edenhofer, O., Pichs-Madruga, R., Sokona, Y., Farahani, E., Kadner, S., Seyboth, K., Adler, A., Baum, I., Brunner, S., Eickemeier, P., Kriemann, B., Savolainen, J., Schlömer, S., von Stechow, C., Zwickel, T., Minx, J., Eds.; Cambridge University Press, Cambridge, UK and New York, NY, USA, 2014; pp 599–670.

(2) Connolly, D.; Mathiesen, B. V.; Ridjan, I. A comparison between renewable transport fuels that can supplement or replace biofuels in a 100% renewable energy system. *Energy* **2014**, *73*, 110–125.

(3) Grube, T.; Doré, L.; Hoffrichter, A.; Hombach, L. E.; Raths, S.; Robinius, M.; Nobis, M.; Schiebahn, S.; Tietze, V.; Schnettler, A.; Walther, G.; Stolten, D. An option for stranded renewables: electrolytic-hydrogen in future energy systems. *Sustain. Energy Fuels* **2018**, *2*, 1500–1515.

(4) Specht, M.; Brellochs, J.; Frick, V.; Stürmer, B.; Zuberbühler, U.; Sterner, M.; Waldstein, G. Speicherung von Bioenergie und erneuerbarem Strom im Erdgasnetz. *Erdöl, Erdgas, Kohle* **2010**, *126*, 342.

(5) Schemme, S.; Samsun, R. C.; Peters, R.; Stolten, D. Power-to-fuel as a key to sustainable transport systems – An analysis of diesel fuels produced from CO_2 and renewable electricity. *Fuel* **2017**, *205*, 198–221.

(6) Bongartz, D.; Doré, L.; Eichler, K.; Grube, T.; Heuser, B.; Hombach, L. E.; Robinius, M.; Pischinger, S.; Stolten, D.; Walther, G.; Mitsos, A. Comparison of light-duty transportation fuels produced from renewable hydrogen and green carbon dioxide. *Appl. Energ.* **2018**, *231*, 757–767.

(7) Burger, J.; Siegert, M.; Ströfer, E.; Hasse, H. Poly(oxymethylene) dimethyl ethers as components of tailored diesel fuel: Properties, synthesis and purification concepts. *Fuel* **2010**, *89*, 3315–3319.

(8) Jacob, E.; Maus, W. Oxymethylenether als potenziell CO_2-neutraler Kraftstoff für saubere Dieselmotoren Teil 2: Erfüllung des Nachhaltigkeitsanspruchs. *MTZ-Motortechnische Zeitschrift* **2017**, *78*, 54–61.

(9) Omari, A.; Heuser, B.; Pischinger, S. Potential of oxymethylenether-diesel blends for ultra-low emission engines. *Fuel* **2017**, *209*, 232–237.

(10) Härtl, M.; Gaukel, K.; Pélerin, D.; Wachtmeister, G. Oxymethylenether als potenziell CO_2-neutraler Kraftstoff für saubere Dieselmotoren Teil 1: Motorenuntersuchungen. *MTZ-Motortechnische Zeitschrift* **2017**, *78*, 52–59.

(11) Deutz, S.; Bongartz, D.; Heuser, B.; Kätelhörn, A.; Schulze Langenhorst, L.; Omari, A.; Walters, M.; Klankermayer, J.; Leitner, W.; Mitsos, A.; Pischinger, S.; Bardow, A. Cleaner production of cleaner fuels: wind-to-wheel – environmental assessment of CO_2-based oxymethylene ether as a drop-in fuel. *Energy Environ. Sci.* **2018**, *11*, 331–343.

(12) Lautenschütz, L.; Oestreich, D.; Seidenspinner, P.; Arnold, U.; Dinjus, E.; Sauer, J. Physico-chemical properties and fuel characteristics of oxymethylene dialkyl ethers. *Fuel* **2016**, *173*, 129–137.

(13) Baranowski, C. J.; Bahmanpour, A. M.; Kröcher, O. Catalytic synthesis of polyoxymethylene dimethyl ethers (OME): A review. *Appl. Catal. B: Environ.* **2017**, *217*, 407–420.

(14) Bertau, M.; Offermanns, H.; Pass, L.; Schmidt, F.; Wernicke, H.-J. *Methanol: The basic chemical and energy feedstock of the future: Asinger's vision today*; Springer-Verlag, Berlin / Heidelberg, 2014.

(15) Zhang, X.; Kumar, A.; Arnold, U.; Sauer, J. Biomass-derived oxymethylene ethers as diesel additives: A thermodynamic analysis. *Energy Procedia* **2014**, *61*, 1921–1924.

(16) Zhang, X.; Oyedun, A. O.; Kumar, A.; Oestreich, D.; Arnold, U.; Sauer, J. An optimized process design for oxymethylene ether production from woody-biomass-derived syngas. *Biomass Bioenergy* **2016**, *90*, 7–14.

(17) Schmitz, N.; Burger, J.; Ströfer, E.; Hasse, H. From methanol to the oxygenated diesel fuel poly (oxymethylene) dimethyl ether: An assessment of the production costs. *Fuel* **2016**, *185*, 67–72.

(18) Ouda, M.; Mantei, F.; Elmehlawy, M.; White, R.; Klein, H.; Fateen, S.-E. Describing oxymethylene ether synthesis based on the application of non-stoichiomsetric Gibbs minimisation. *Reac. Chem. Eng.* **2018**, *3*, 277–292.

(19) Ouda, M.; Mantei, F.; Hesterwerth, K.; Bargiacchi, E.; Klein, H.; White, R. J. A hybrid description and evaluation of oxymethylene dimethyl ethers synthesis based on the endothermic dehydrogenation of methanol. *React. Chem. Eng.* **2018**, *3*, 676–695.

(20) Mahbub, N.; Oyedun, A. O.; Kumar, A.; Oestreich, D.; Arnold, U.; Sauer, J. A life cycle assessment of oxymethylene ether synthesis from biomass-derived syngas as a diesel additive. *J. Cleaner Prod.* **2017**, *165*, 1249–1262.

(21) Kuhnert, C.; Albert, M.; Breyer, S.; Hahnenstein, I.; Hasse, H.; Maurer, G. Phase Equilibrium in Formaldehyde Containing Multicomponent Mixtures: Experimental Results for Fluid Phase Equilibria of (Formaldehyde + (Water or Methanol) + Methylal)) and (Formaldehyde + Water + Methanol + Methylal) and Comparison with Predictions. *Ind. Eng. Chem. Res.* **2006**, *45*, 5155–5164.

(22) Burger, J.; Ströfer, E.; Hasse, H. Production process for diesel fuel components poly(oxymethylene) dimethyl ethers from methane-based products by hierarchical optimization with varying model depth. *Chem. Eng. Res. Des.* **2013**, *91*, 2648–2662.

(23) Weidert, J.-O.; Burger, J.; Renner, M.; Blagov, S.; Hasse, H. Development of an integrated reaction-distillation process for the production of methylal. *Ind. Eng. Chem. Res.* **2017**, *56*, 575–582.

(24) Burre, J.; Bongartz, D.; Mitsos, A. Production of Oxymethylene Dimethyl Ether from Hydrogen and Carbon Dioxide – Part II: Modeling and Analysis for $OME_{3\text{-}5}$. *Submitted for publication* **2019**,

(25) Burre, J.; Bongartz, D. AspenPlus implementations of process models for the production of OME_n from H_2 and CO_2. `http://permalink.avt.rwth-aachen.de/?id=661625`, 2019.

(26) Walker, J. F. *Formaldehyde*; Reinhold Publishing Corporation., New York, 1944.

(27) Niethammer, B.; Wodarz, S.; Betz, M.; Haltenort, P.; Oestreich, D.; Hackbarth, K.; Arnold, U.; Otto, T.; Sauer, J. Alternative Liquid Fuels from Renewable Resources. *Chem. Ing. Tech.* **2018**, *90*, 99–112.

(28) Thenert, K.; Beydoun, K.; Wiesenthal, J.; Leitner, W.; Klankermayer, J. Ruthenium-Catalyzed Synthesis of Dialkoxymethane Ethers Utilizing Carbon Dioxide and Molecular Hydrogen. *Angew. Chem. Int. Ed.* **2016**, *55*, 12266–12269.

(29) Schieweck, B. G.; Klankermayer, J. Tailor-made Molecular Cobalt Catalyst System for the Selective Transformation of Carbon Dioxide to Dialkoxymethane Ethers. *Angew. Chem. Int. Ed.* **2017**, *56*, 10854–10857.

(30) Pontzen, F.; Liebner, W.; Gronemann, V.; Rothaemel, M.; Ahlers, B. CO_2-based methanol and DME–Efficient technologies for industrial scale production. *Catal. Today* **2011**, *171*, 242–250.

(31) Van-Dal, É. S.; Bouallou, C. Design and simulation of a methanol production plant from CO_2 hydrogenation. *J. Cleaner Prod.* **2013**, *57*, 38–45.

(32) Otto, A. Chemical, procedural and economic evaluation of carbon dioxide as feedstock in the chemical industry. Ph.D. thesis, RWTH Aachen University, 2015.

(33) ASTM International, *Standard Specification for Methanol (Methyl Alcohol)*; ASTM D1152-97, 1997.

(34) Reuss, G.; Disteldorf, W.; Gamer, A.; Hilt, A. Formaldehyde. In *Ullmann's Encyclopedia or Industrial Chemistry*; Wiley-VCH, Weinheim, Germany, 2012; pp 735–768.

(35) Sperber, H. Herstellung von Formaldehyd aus Methanol in der BASF. *Chem. Ing. Tech.* **1969**, *41*, 962–966.

(36) Albert, M.; Hahnenstein, I.; Hasse, H.; Maurer, G. Vapor-liquid and liquid-liquid equilibria in binary and ternary mixtures of water, methanol, and methylal. *J. Chem. Eng. Data* **2001**, *46*, 897–903.

(37) Enk, E.; Knörr, F.; Spes, H. Process for the recovery of methanol free and water free methylal. Patent US 3222262. 1965.

(38) Müller, W. H. E.; Kaufhold, M. Process for the recovery of pure methylal from methanol-methylal mixtures. Patent US 4385965. 1983.

(39) Carretier, E.; Moulin, P.; Beaujean, M.; Charbit, F. Purification and dehydration of methylal by pervaporation. *J. Membr. Sci.* **2003**, *217*, 159–171.

(40) Drunsel, J.-O. Entwicklung von Verfahren zur Herstellung von Methylal und Ethylal. Ph.D. thesis, TU Kaiserslautern, 2012.

(41) Hasse, H.; Drunsel, J.-O.; Burger, J.; Schmidt, U.; Renner, M.; Blagov, S. Process for the production of pure methylal. Patent US 9346727 B2. 2016.

(42) Green, S. J.; Vener, R. E. Vapor-liquid equilibria of formaldehyde-methanol-water. *Ind. Eng. Chem.* **1955**, *47*, 103–109.

(43) Maurer, G. Vapor-liquid equilibrium of formaldehyde- and water-containing multicomponent mixtures. *AIChE J.* **1986**, *32*, 932–948.

(44) Fredenslund, A.; Jones, R. L.; Prausnitz, J. M. Group-contribution estimation of activity coefficients in nonideal liquid mixtures. *AIChE J.* **1975**, *21*, 1086–1099.

(45) Hasse, H.; Hahnenstein, I.; Maurer, G. Revised vapor-liquid equilibrium model for multicomponent formaldehyde mixtures. *AIChE J.* **1990**, *36*, 1807–1814.

(46) Hahnenstein, I.; Hasse, H.; Kreiter, C. G.; Maurer, G. 1 H-and 13 C-NMR-spectroscopic study of chemical equilibria in solutions of formaldehyde in water, deuterium oxide, and methanol. *Ind. Eng. Chem. Res.* **1994**, *33*, 1022–1029.

(47) Albert, M.; Garcia, B. C.; Kreiter, C.; Maurer, G. Vapor-liquid and chemical equilibria of formaldehyde-water mixtures. *AIChE J.* **1999**, *45*, 2024–2033.

(48) Albert, M.; Garcia, B. C.; Kuhnert, C.; Peschla, R.; Maurer, G. Vapor-liquid equilibrium of aqueous solutions of formaldehyde and methanol. *AIChE J.* **2000**, *46*, 1676.

(49) Hasse, H. Dampf-Flüssigkeits-Gleichgewichte, Enthalpien und Reaktionskinetik in formaldehydhaltigen Mischungen. Ph.D. thesis, TU Kaiserslautern, 1990.

(50) Liu, Y.-Q.; Hasse, H.; Maurer, G. Enthalpy change on vaporization of aqueous and methanolic formaldehyde solutions. *AIChE J.* **1992**, *38*, 1693–1702.

(51) Albert, M.; Hasse, H.; Kuhnert, C.; Maurer, G. New Experimental Results for the Vapor-Liquid Equilibrium of the Binary System (Trioxane + Water) and the Ternary System (Formaldehyde + Trioxane + Water). *J. Chem. Eng. Data* **2005**, *50*, 1218–1223.

(52) Schmitz, N.; Friebel, A.; von Harbou, E.; Burger, J.; Hasse, H. Liquid-liquid equilibrium in binary and ternary mixtures containing formaldehyde, water, methanol, methylal, and poly (oxymethylene) dimethyl ethers. *Fluid Phase Equilib.* **2016**, *425*, 127–135.

(53) Abrams, D. S.; Prausnitz, J. M. Statistical thermodynamics of liquid mixtures: a new expression for the excess Gibbs energy of partly or completely miscible systems. *AIChE J.* **1975**, *21*, 116–128.

(54) Detcheberry, M.; Destrac, P.; Meyer, X.-M.; Condoret, J.-S. Phase equilibria of aqueous solutions of formaldehyde and methanol: Improved approach using UNIQUAC coupled to chemical equilibria. *Fluid Phase Equilib.* **2015**, *392*, 84–94.

(55) Ott, M.; Fischer, H. H.; Maiwald, M.; Albert, K.; Hasse, H. Kinetics of oligomerization reactions in formaldehyde solutions: NMR experiments up to 373 K and thermodynamically consistent model. *Chem. Eng. Process.* **2005**, *44*, 653–660.

(56) Drunsel, J.-O.; Renner, M.; Hasse, H. Experimental study and model of reaction kinetics of heterogeneously catalyzed methylal synthesis. *Chem. Eng. Res. Des.* **2012**, *90*, 696–703.

(57) Albert, M. Thermodynamische Eigenschaften formaldehydhaltiger Mischungen. Ph.D. thesis, TU Kaiserslautern, 1999.

(58) Ott, M. Reaktionskinetik und Destillation formaldehydhaltiger Mischungen. Ph.D. thesis, TU Kaiserslautern, 2004.

(59) Kuhnert, C. Dampf-Flüssigkeits-Gleichgewichte in mehrkomponentigen formaldehydhaltigen Systemen. Ph.D. thesis, TU Kaiserslautern, 2004.

(60) Auerbach, F.; Barschall, H. *Studien über Formaldehyd I. Formaldehyd in wässriger Lösung*; Julius Springer, Berlin, 1905.

(61) Natta, G.; Baccaredda, M. *Giorn. di Chimica Ind. et Applicata* **1933**, 273–281.

(62) Soave, G. Equilibrium constants from a modified Redlich-Kwong equation of state. *Chem. Eng. Sci.* **1972**, *27*, 1197–1203.

(63) Huron, M.-J.; Vidal, J. New mixing rules in simple equations of state for representing vapour-liquid equilibria of strongly non-ideal mixtures. *Fluid Phase Equilib.* **1979**, *3*, 255–271.

(64) van den Bussche, K.; Froment, G. A steady-state kinetic model for methanol synthesis and the water gas shift reaction on a commercial $Cu/ZnO/Al_2O_3$ catalyst. *J. Catal.* **1996**, *161*, 1–10.

(65) Zhang, J.; Shi, M.; Fang, D.; Liu, D. Reaction kinetics of the production of polyoxymethylene dimethyl ethers from methanol and formaldehyde with acid cation exchange resin catalyst. *Reac. Kinet. Mech. Catal.* **2014**, *113*, 459–470.

(66) König, D. H.; Baucks, N.; Dietrich, R.-U.; Wörner, A. Simulation and evaluation of a process concept for the generation of synthetic fuel from CO_2 and H_2. *Energy* **2015**, *91*, 833–841.

(67) Bejan, A.; Tsatsaronis, G.; Moran, M. *Thermal Design & Optimization*; John Wiley & Sons, Inc., New York, 1996.

Abstract Graphic